Distinctive orbital anisotropy observed in the nematic state of a FeSe thin film

Y. Zhang, M. Yi, Z.-K. Liu, W. Li, J. J. Lee, R. G. Moore, M. Hashimoto, M. Nakajima, H. Eisaki, S.-K. Mo, Z. Hussain, T. P. Devereaux, Z.-X. Shen, and D. H. Lu

Phys. Rev. B **94**, 115153 — Published 26 September 2016

DOI: 10.1103/PhysRevB.94.115153

Distinctive orbital anisotropy observed in the nematic state of FeSe thin film

Y. Zhang,[1,2] M. Yi,[1,3] Z. -K Liu,[1,3] W. Li,[1] J. J. Lee,[1,3] R. G. Moore,[1] M. Hashimoto,[4] M. Nakajima,[5,6] H. Eisaki,[5,6] S. -K. Mo,[2] Z. Hussain,[2] T. P. Devereaux,[1,3] Z. -X. Shen,[1,3,*] and D. H. Lu[4,†]

[1]*Stanford Institute for Materials and Energy Sciences, SLAC National Accelerator Laboratory, 2575 Sand Hill Road, Menlo Park, California 94025, USA*
[2]*Advanced Light Source, Lawrence Berkeley National Laboratory, Berkeley, California 94720, USA*
[3]*Geballe Laboratory for Advanced Materials, Departments of Physics and Applied Physics, Stanford University, Stanford, California 94305, USA*
[4]*Stanford Synchrotron Radiation Lightsource, SLAC National Accelerator Laboratory, 2575 Sand Hill Road, Menlo Park, California 94025, USA*
[5]*National Institute of Advanced Industrial Science and Technology, Tsukuba, Ibaraki 305-8568, Japan*
[6]*JST, Transformative Research-Project on Iron Pnictides, Tokyo, 102-0075, Japan*

(Dated: September 6, 2016)

Nematic state, where a system is translationally invariant but breaks rotational symmetry, has drawn great attentions recently due to the experimental observations of such a state in both cuprates and iron-based superconductors. The origin of nematicity and its possible tie to the pairing mechanism of high-T_c, however, still remains controversial. Here, we studied the electronic structure of multilayer FeSe film using angle-resolved photoemission spectroscopy (ARPES). The band reconstruction in the nematic state is clearly delineated. We found that the energy splitting between d_{xz} and d_{yz} bands shows non-monotonic distribution in momentum space. From the Brillouin zone center to the Brillouin zone corner, the magnitude of splitting first decreases, then increases, and finally reaches the maximum value of ∼70 meV. Moreover, besides the d_{xz} and d_{yz} bands, band splitting was also observed on the d_{xy} bands with a comparable energy scale around 45 meV. Our results suggest that the electronic anisotropy in the nematic state cannot be explained by a simple on-site ferro-orbital order. Instead, strong anisotropy exists in the hopping of all d_{xz}, d_{yz}, and d_{xy} orbitals, the origin of which holds the key to a microscopic understanding of the nematicity in iron-based superconductors.

PACS numbers: 74.25.Jb,74.70.Xa,79.60.-i,73.21.Ac

INTRODUCTION

High-T_c superconductivity often occurs in proximity to symmetry breaking states, whose origins are intimately related to the pairing mechanism of superconductivity. Among all these symmetry-breaking states, nematic state, in which electrons break the rotational symmetry without breaking the translational symmetry, has recently drawn great attentions [1, 2]. It was observed in proximity to high-T_c superconductivity in both cuprates and iron-based superconductors [3–9], and the quantum fluctuation near a nematic quantum critical point was proposed to be critical for high-T_c superconductivity [10, 11].

In iron-based superconductors, the nematic state develops simultaneously with a structural transition from tetragonal to orthorhombic structure[2]. A magnetic transition into a collinear antiferromagnetic (CAF) order follows simultaneously or at a lower temperature [12]. In order to explain the nematic state, most theories emphasize the importance of orbital/spin fluctuations or their strong coupling, in connection with the multi-orbital and correlated nature of iron-based superconductors [13–19]. The key debates among these theories lie in which fluctuation dominates at high temperature and what relationship the nematic and magnetic states have. Under the spin-nematic scenario [18, 19], both the nematic and magnetic states share the same origin, namely the spin fluctuation. It has been proposed that the spin fluctuation could break the C4 rotational symmetry spontaneously by peaking either at $(0, \pi)$ or $(\pi, 0)$, resulting in a spin-nematic state. Such a state occurs prior to the magnetic ordered state and is responsible for the structural transition through magnetic-elastic coupling. On the other hand, in the orbital-ordering scenario, the nematic and magnetic states are considered to be separate [13–15]. The orbital fluctuation dominates at high temperature and breaks the C4 rotational symmetry by triggering a d_{xz}/d_{yz} ferro-orbital ordering. Subsequently, at a lower temperature, the orbital ordering further enhances the spin fluctuation and its anisotropy, which results in a magnetic transition under sufficiently strong coupling between the spin and orbital/lattice degrees of freedom.

The origin of nematicity is crucial for understanding the nature of competing phases in high-T_c superconductors and needs to be examined experimentally. However, clear experimental delineation of the nematic state has always been challenging. In most iron-pnictide compounds, the nematic and magnetic states are strongly intertwined with each other, preventing us from probing the intrinsic properties of nematic state. FeSe is an ideal system. Bulk FeSe shows a structural transition at ∼90 K, where the lattice breaks the C4 rotational symmetry. However, no long-range magnetic order has been observed down to the lowest experimental temperature[20–22]. Its electronic structure has been studied by several angle-resolved photoemission spectroscopy (ARPES) groups [23–27]. The energy splitting between the d_{xz} and d_{yz} bands has been observed in the nematic state and the importance of d_{xz} and d_{yz} orbital ordering has been discussed. In this paper,

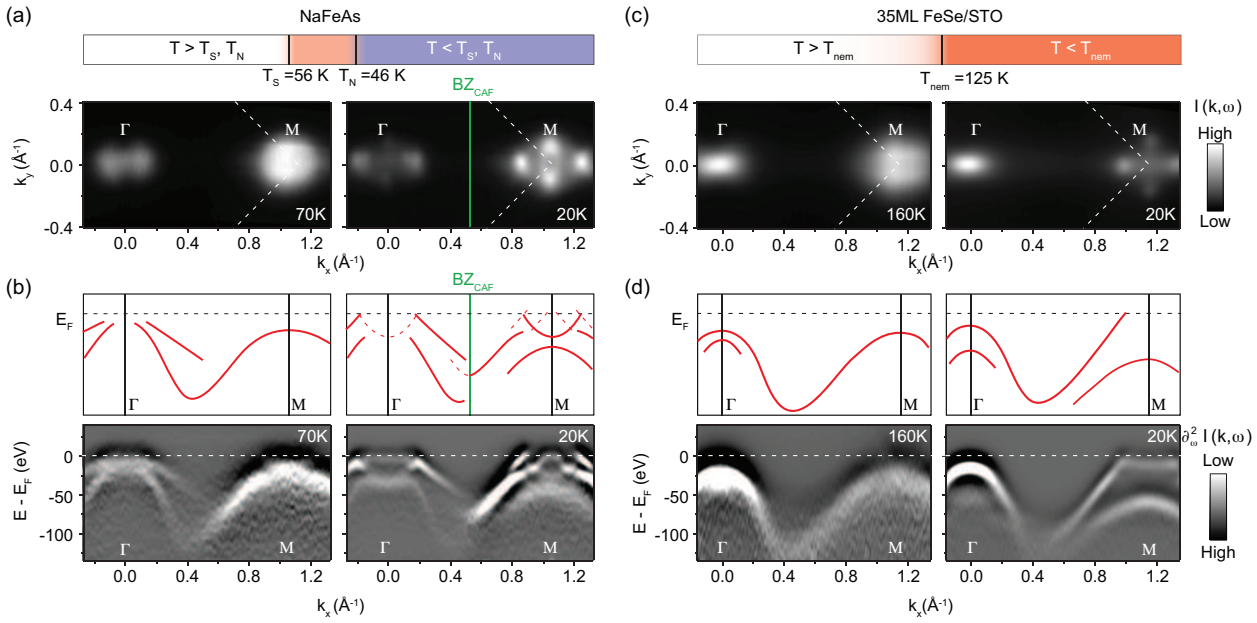

FIG. 1: (color online) Absence of magnetic order in FeSe thin film. (a) The Fermi surface mapping taken at 70 K and 20 K in NaFeAs. The Brillouin zone (BZ) boundary in the magnetic state is shown by green sold line. The structural transition temperature and magnetic transition temperature are abbreviated as T_s and T_N, respectively. (b) The second derivative photoemission intensity distribution taken along the Γ-M direction. The main (solid line) and folded (dashed line) bands are illustrated in the upper panels. (c) and (d) are the corresponding data taken on 35ML FeSe film at 160 K and 20 K, respectively. The data were taken with 38 eV photons with the k_z near the Γ point. The nematic transition temperature is abbreviated as T_{nem}.

we present our ARPES studies on the 35 monolayers (35ML) FeSe film grown on $SrTiO_3$.The nematic transition temperature (T_{nem}) is around 125 K and the band reconstruction in the nematic state is clearly delineated. We find that the energy splitting between the d_{xz} and d_{yz} bands shows non-trivial momentum dependence. Specifically, from the Brillouin zone (BZ) center (Γ) to the BZ corner (M), the energy splitting of bands first decreases, then increases, and finally achieves the maxiumum value of ∼70 meV at M. Moreover, three electron bands were clearly resolved near M, demonstrating that the d_{xy} bands also reconstruct in the nematic state with an energy scale around 45 meV. Our results have strong implications for theories aiming to understand the nature of nematic state. The momentum dependence of the d_{xz} and d_{yz} energy splitting and the reconstruction of d_{xy} exclude the simple on-site ferro-orbital ordering as a driving force of nematicity. Instead, the hopping anisotropy of all the d_{xz}, d_{yz} and d_{xy} orbitals should play a more important role.

EXPERIMENTAL

FeSe films were grown on high quality Nb-doped (0.05% wt) $SrTiO_3$ (100) substrates. TiO_2 terminated atomic flat surface were prepared by degassing at 450 °C for several hours and subsequently annealing at 900 °C for 20 min. The growth was carried out under Se-rich condition with a Se/Fe flux ratio of 3 ∼ 4. Substrate temperatures were kept at 380 °C during the growth. The films were subsequently annealed at 450 °C for four hours immediately after growth. ARPES measurements were performed at the beamline 5-4 of Stanford Synchrotron Radiation Lightsource (SSRL) and the beamline 10.0.1 of Advanced Light Source (ALS). All data were taken with Scienta R4000 electron analyzers. The overall energy resolution was 5 ∼ 10 meV depending on the photon energy, and the angular resolution was 0.3 °. For the ARPES measurements at SSRL, the films were transferred from the growth chamber to the ARPES chamber via a vacuum suitcase with a pressure better than 1×10^{-9} torr. For the ARPES measurements at ALS, each film was capped with a Se layer of 25 nm thick to protect the thin film during sample transfer. The film was then heated up to 400 °C to decap the Se capping layer in the ARPES chamber. All the samples were measured in ultra-high vacuum with a base pressure better than 3×10^{-11} torr.

RESULTS

The CAF order of iron-based superconductors breaks the translational symmetry [12]. As a result, the unit cell rotates 45 degrees and doubles in size. The electronic manifestation for such a translational symmetry breaking is the band folding in momentum space. We take NaFeAs as an example, whose structural transition temperature (T_s) and magnetic transition temperature (T_N) are around 56 and 46 K, respectively [28]. As shown in Fig. 1(a), the Fermi surface of NaFeAs at 70 K

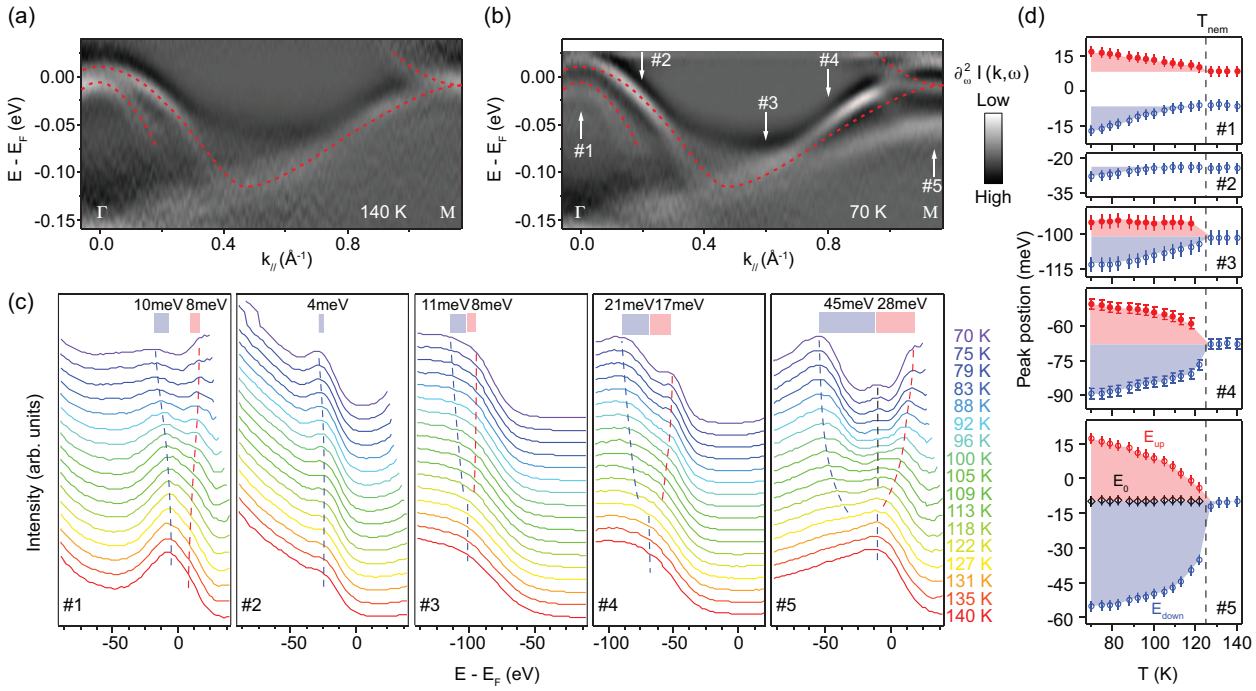

FIG. 2: (color online) Nontrivial momentum dependence of the band reconstruction. (a) The second derivative photoemission intensity distribution taken on 35ML FeSe film along the Γ-M direction at 140 K. (b) is the same as panel a, but taken at 70 K. The red dashed lines show the high temperature band dispersion extracted from panel a. The data were taken with 25 eV photons. The hole bands show moderate k_z dispersion and cross E_F when the 25 eV photon energy selects with the k_z between Γ and Z. (c) The temperature dependence of the energy distribution curves (EDCs) taken at five different momenta, after the division of Fermi-Dirac function. The peak positions are determined via a combination of spectral weight maximum and second derivative curve minimum. The top red and blue bars illustrate the energy scale of the band shift. We note that, there is constant finite constant energy splitting between the inner and outer hole bands at Γ above T_{nem}, which could be due to spin-orbit coupling. (d) The temperature dependence of the band positions extracted from the data in panel c.

consists of hole pockets around Γ and electron pockets around M [29, 30]. In CAF ordered state, the bands around Γ and M fold onto each other [Fig. 1(b)], and the Fermi surface sheets reconstruct so that they are symmetric with respect to the magnetic BZ boundary [Fig. 1(a)]. We note that, without translational symmetry breaking, the size of unit cell remains the same and the bands do not fold. Therefore, the band folding observed here is a spectroscopic evidence for long-range magnetic order in NaFeAs, indicting a translational symmetry breaking.

For 35ML FeSe film, such a band folding behavior is clearly absent. Figure 1(c) shows the Fermi surface mappings taken on 35ML FeSe film. The Fermi surface at 160 K consists of small hole and electron pockets, which is similar to that of NaFeAs. At 20 K, the Fermi surface of FeSe thin film only reconstructs around the M point and forms four intense propeller-like pockets. The strong discrepancy of Fermi surface between Γ and M indicates the absence of band folding behavior. Fig. 1(d) shows the measured dispersion taken along the Γ-M direction. None of the bands observed at 20 K could be attributed to a band folding. Further evidences come from the absence of spin density wave (SDW) gap. In contrast to NaFeAs, where the band dispersions break into segments in the SDW state due to SDW gap opening [Fig. 1(b)], the bands disperse continuously in FeSe and no SDW gap is observed [Fig. 1(d)]. All these results unambiguously demonstrate the absence of magnetic order in 35ML FeSe film, which is also consistent with the data taken from FeSe single crystal showing no static magnetic order down to the lowest temperature [20–27]. Note that, no surface reconstruction has been observed in FeSe thin film and the bands show moderate k_z dispersion in ARPES studies [31, 32]. Therefore, the ARPES spectra reflect the intrinsic properties of FeSe thin film.

The sample in the nematic state consists of two perpendicular domains due to the breaking of C4 rotational symmetry. As shown in previous ARPES studies on detwinned $Ba(Fe_{1-x}Co_x)_2As_2$ and NaFeAs [5, 29, 30], the d_{xz} and d_{yz} bands shift oppositely along two perpendicular Fe-Fe directions in a single domain. Such band shift manifests itself as an energy splitting between the d_{xz} and d_{yz} bands in the twinned sample due to the superposition of photoemission signals from two perpendicular domains. In FeSe thin film, the most pronounced band reconstruction is the energy splitting between the d_{xz} and d_{yz} bands [Fig. 1(d)], which is similar to what have been observed in iron-pnictide compounds [5, 29, 30]. However, without the interference of long-range magnetic order, the band reconstruction is much simpler and more distinguishable in FeSe. For example, the whole d_{yz} hole-like band

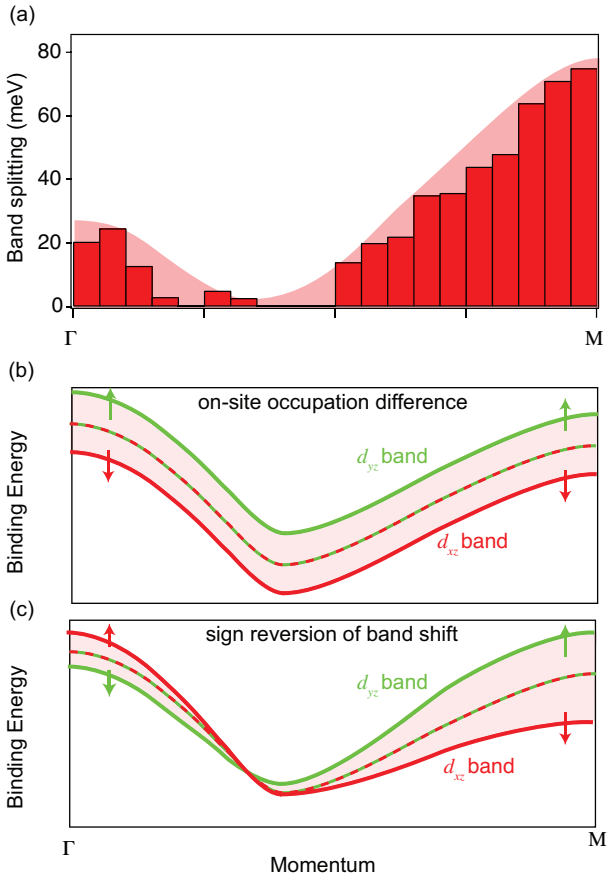

FIG. 3: (color online) Momentum dependence of the band splitting along Γ-M direction in the nematic state. (a) Momentum dependence of the band splitting between d_{xz} and d_{yz} bands along Γ-M direction. The shaded area is illustrated to guide the eye. (b) Illustration of the d_{xz} and d_{yz} band splitting in the nematic state considering the on-site occupation difference between d_{xz} and d_{yz} bands. (c) Illustration of the d_{xz} and d_{yz} band splitting in the nematic state considering the band shift reversion from Γ to M.

is observed shifting up to above E_F in FeSe, while in NaFeAs, only a small section of this band can be observed due to the SDW gap opening associated with the CAF order. Therefore, FeSe is an ideal system for us to quantitatively study the band reconstruction in the nematic state.

We overlaid the high temperature band dispersion extracted from Fig. 2(a) (the red dashed lines) on top of the low temperature spectra image, as shown in Fig. 2(b). The band reconstruction at M is much more pronounced than that at Γ. Figure 2(c) shows the detailed temperature evolution of the energy distribution curves (EDCs) taken at five different momenta as indicated in Fig. 2(b). The band positions at each temperature were determined through peak fittings and plotted in Fig. 2(d). All bands start to shift at ~125 K, which we interpret as the T_{nem} for 35ML FeSe film, as this is the temperature that symmetry breaking between the d_{xz} and d_{yz} orbitals begins. The T_{nem} of 35ML FeSe film is higher than that of FeSe single crystal. The enhancement of T_{nem} may originate from the lattice strain in FeSe thin film [33]. When the thickness of the film decreases, the $SrTiO_3$ substrate induces tensile strain to the FeSe thin film. As a result, the general electronic correlation, orbital and spin fluctuations all changes due to the changes of bond angle and bond length. We note that spin orbital coupling induces a finite band splitting at Γ even above T_{nem}. To characterize the C4 rotational symmetry breaking between d_{xz} and d_{yz}, only the additional band splitting below T_{nem} is considered. We then determines the magnitude of band splitting between d_{xz} and d_{yz} bands at different momenta. We found that the magnitude of band splitting is strongly momentum-dependent and changes non-monotonically from Γ to M. More specifically, it is around 20 meV at Γ, and decreases to its minimum value at the momentum slightly away from Γ, then increases towards M, and finally reaches its maximum value of 70 meV at M [Fig. 3(a)].

The energy splitting between d_{xz} and d_{yz} has been taken as an evidence for the existence of ferro-orbital ordering in the nematic state. However, the d_{xz} and d_{yz} ferro-orbital ordering is normally considered as an on-site occupation difference between the d_{xz} and d_{yz} orbital. Such an occupation difference would result in a d_{xz} and d_{yz} band splitting that is momentum independent [Fig. 3(b)], which is inconsistent with our observation. Alternatively, the middle parts of the d_{xz} and d_{yz} bands remain unchanged through the nematic transition [Fig. 3(a)], indicating that the band shift might change sign when going from Γ to M. As shown in Fig. 3(c), such band shift could well explain the observed non-monotonic momentum dependence of the energy splitting. Consistently, the sign reversal of the band shift at Γ and M has been confirmed recently by the ARPES study on detwinned FeSe single crystal [27].

Because the bands reconstruction occurs primarily near the M point, Fig. 4 focuses on the temperature dependence of photoemission spectra taken around the M point in 35ML FeSe film. The Fermi surface is ellipse-like at 160K. The C2 symmetry of Fermi surface above T_{nem} is originated from matrix element effect and the glide-mirror symmetry of FeSe plane [34]. Upon entering the nematic state, the Fermi surface shrinks along the k_x direction and finally evolves into two small Fermi pockets [Fig. 4(a)]. The band reconstruction could be tracked by the energy positions of the hole-like band tops and the electron-like band bottoms [Fig. 4(b)]. The band tops and bottoms are degenerate at 160 K, respecting the C4 symmetry of the tetragonal lattice. Upon lowering the temperature, the hole and electron bands shift consistently and splits into three separate branches: one branch (E_{up}) shift upwards above the Fermi energy (E_F) and another branch (E_{down}) shift downwards to higher binding energy. In the middle, a shallow electron band was observed at low temperature, whose band bottom (E_0) is nearly unchanged with temperature.

We then determine how the bands reconstruct near the M point. The d_{xz}, d_{yz}, and d_{xy} orbitals construct two pairs of hole-like and electron bands near the M point [Figs. 4(c1) and 4(d1)]. The hole-like band top and electron band bottom are degenerate at the M point. Such degeneracy can only be lifted by a breaking of glide-mirror symmetry or spin-orbital

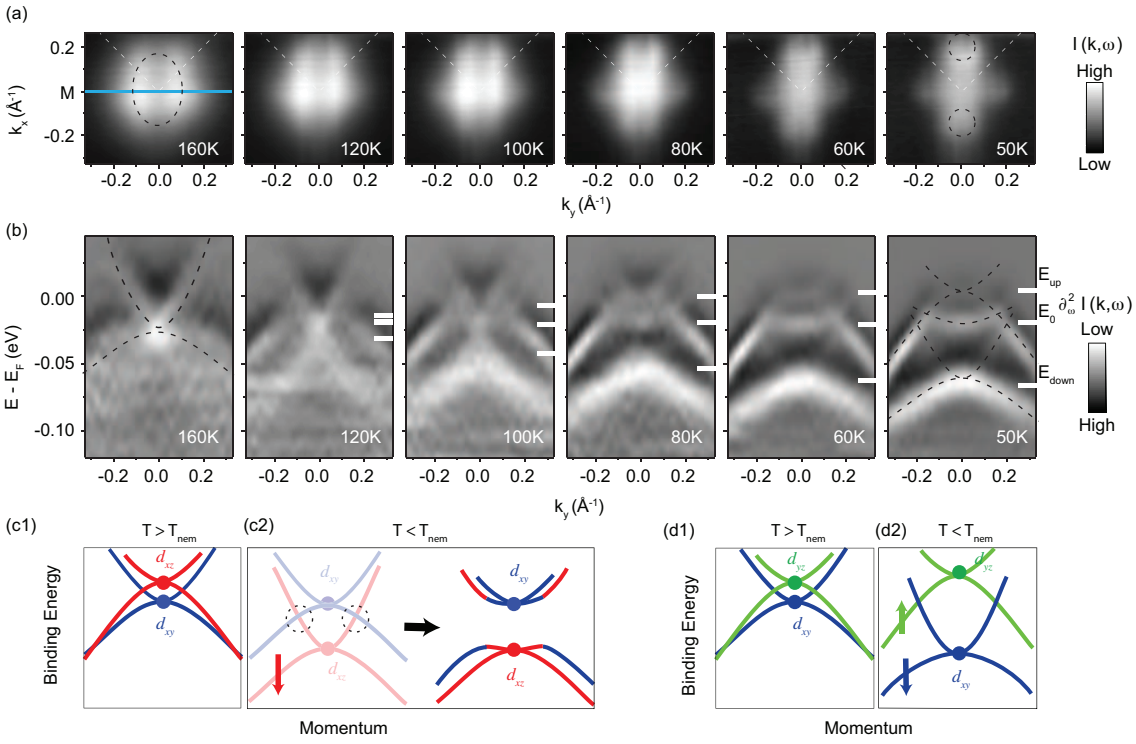

FIG. 4: (color online) Band structure reconstruction near the M point in the nematic state. (a) Temperature dependence of the Fermi surface mapping near the M point. (b) Temperature dependence of the second derivative of photoemission intensity distribution taken along the Γ-M direction. The cut direction is shown by the cyan solid line in panel a. The solid lines with different colors mark the energy positions of either the band tops of hole-like bands or bottoms of electron-like bands. The dashed solid lines are the guide to the eyes for the band dispersion and Fermi surface. (c) Schematic of the band shift and hybridization of the d_{xz} and d_{xy} bands near the M_Y point. (d) Schematic of the band shift of the d_{yz} and d_{xy} bands near the M_X point. The data were taken with 38 eV photons.

coupling. For FeSe thin film, there is no experimental evidence for a glide-mirror symmetry breaking and the effect of spin-orbital coupling is weak near the M point. Therefore, the degeneracy between the hole-like band top and electron band bottom should remain unchanged when entering the nematic state. However, for the middle electron band, there is no hole-like band that is associated with it. In the nematic state, the d_{yz} and d_{xz} hole-like bands shift upward and downward respectively (Figs. 2 and 3). According to the band symmetry, once the d_{xz} electron band shifts below the d_{xy} hole-like band, hybridization gap would open between them, resulting in an energy separation between electron band bottom and hole-like band top [35, 36][Fig. 4(c2)]. This is the only possible schematic in which an electron band bottom is observed and there is no associated hole-like band top. Moreover, the band dispersion of the middle electron band flattens in the nematic state, which can be well explained by the hybridization gap opening between the d_{xz} electron band and the d_{yz} hole band [Fig. 4(c2)]. Therefore, the middle electron band is most likely originated from the hybridized d_{xz} and d_{xy} bands. Contrary to the d_{xz} electron band, when the d_{yz} electron band shifts up, there is no band hybridization and the electron band bottom remains degenerate with the hole-like band top [Fig. 4(d2)]. The upper electron band can be then attributed to the d_{yz} electron band. For the deeper electron band, previous ARPES studies attribute it to the d_{xz} band [23–25]. However, as shown here in FeSe thin film, the d_{xz} and d_{yz} orbitals contribute the middle and upper electron bands, suggesting that the deeper electron band has to be originated from the d_{xy} orbital. Its band bottom shifts downwards in the nematic state [Fig. 4(d2)]. We note that, the middle flat electron band has not been observed in FeSe single crystal [23–27]. Recently, it has been shown that the middle electron band is above E_F in FeSe single crystal and hence cannot be observed [37]. By doping electrons, the middle electron band shifts downward and emerges at certain doping level. The observation of three electron bands in FeSe thin film complements the previous ARPES studies on FeSe and is crucial for understanding the complex band reconstruction in the nematic state.

We then illustrate the band reconstruction near the M point in Figs. 5(a) - 5(d). We first consider the band structure in one-Fe BZ for simplicity. The d_{yz} and d_{xz} bands hybridize with the d_{xy} bands near M_X and M_Y, respectively, forming two pairs of electron and hole-like bands [38]. In the nematic state, the d_{yz} band shifts up around the M_X point. As a result, the electron pocket shrinks along one direction and eventually

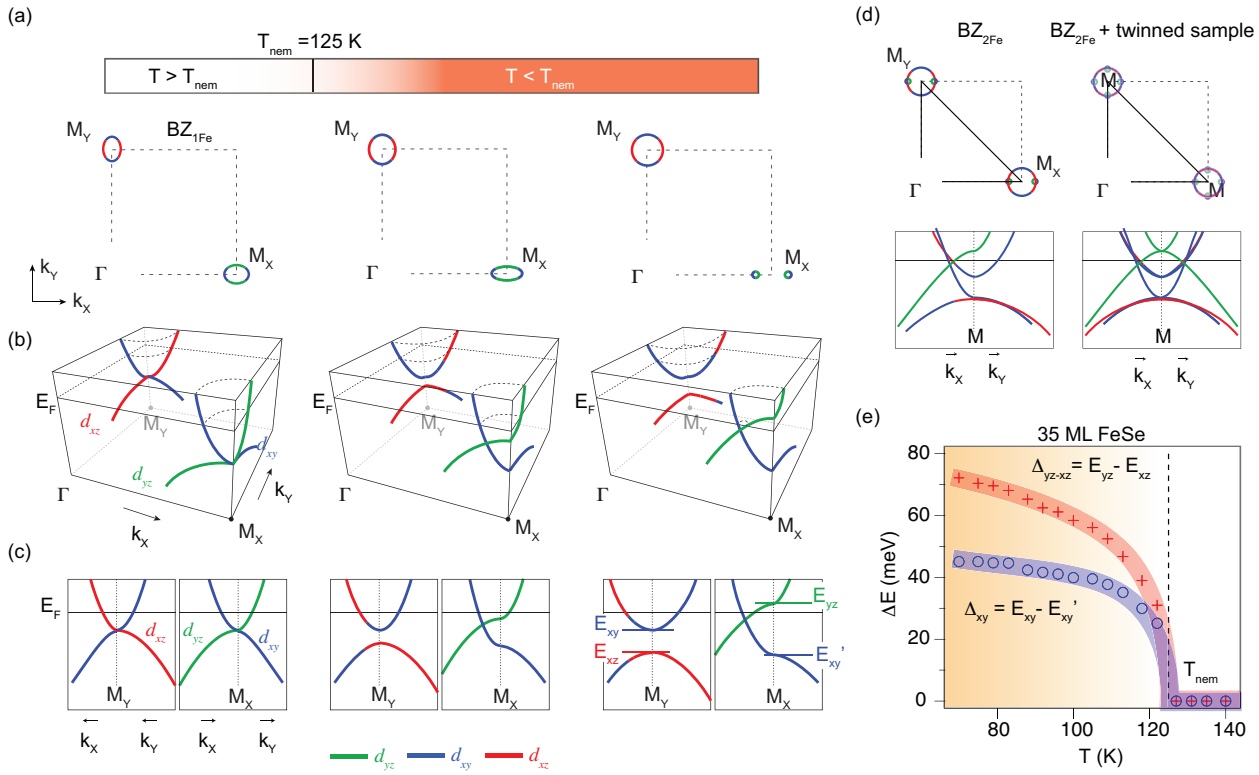

FIG. 5: (color online) Schematics of band reconstruction near the M point through the nematic transition. Illustration of the reconstruction of Fermi surface (a) and band structure (b) and (c) around the M point in one-Fe BZ. For simplicity, we neglect the hole bands and associated hole pockets near the zone center the Γ point. The bands are stretched in three-dimensional plots for a better view of the band reconstruction. (d) Illustration of the low temperature electronic structure in two-Fe BZ by folding the corresponding bands between M_X and M_Y (left panel) and in twinned sample by overlapping the bands in two perpendicular domains (right panel). (e) Temperature dependence of the energy splitting extracted from the band tops and bottoms at the M point.

evolves into two small Fermi pockets. On the contrary, around the M_Y point, the d_{xz} band shifts downwards and opens a hybridization gap with the d_{xy} band, which enlarges the electron pocket at the M_Y point. This enlargement could also be considered as a volume compensation for the shrink of electron pocket at the M_Y point. We then folded these bands back into the two-Fe BZ and obtained the reconstructed Fermi surface and band structure in Fig. 5(d). Moreover, due to the sample twinning effect, the experimental band structure is a superposition of bands from two perpendicular domains [4]. Taking this effect into consideration, Fig. 5(d) reproduces the observed propeller-like Fermi pockets and the band splitting at the M point very well. We note that part of the circular electron pocket is constructed by the d_{xy} orbital [Fig. 5(d)], whose photoemission matrix elements is much weaker than the d_{xz} and d_{yz} orbitals[5]. Therefore, the circular electron pocket appears missing in the Fermi surface mapping in Fig. 4(a).

One intriguing feature in Fig. 5(a) is that, the d_{xy} electron band shifts towards higher binding energy near the M_X point resulting in a finite energy splitting between the d_{xy} bands at the M_X and M_Y points ($\Delta_{xy} = E_{xy}$ - $E_{xy'}$). Such an energy splitting is around 45 meV, which is comparable with the 70 meV energy splitting between the d_{xz} and d_{yz} bands ($\Delta_{yz-xz} = E_{yz}$ E_{xz}). This result suggests that the d_{xy} orbital also plays an important role in driving nematicity. Fig. 5(e) shows the temperature dependence of Δ_{yz-xz} and Δ_{xy}. The order parameter like behavior suggests that both d_{xz}/d_{yz} and d_{xy} energy splitting could be viewed as a pivotal characteristic property of the nematic state. Their origin holds the key in understanding the mechanism of the nematicity.

DISCUSSIONS

The observed band reconstruction and its distinctive distribution in the momentum space put strong constrains on theories. Our results do not favor the spin-nematic scenario, because no signature of long-range magnetic ordering, i.e., band folding, was observed in FeSe down to the lowest measurement temperature (20 K), even though the T_{nem} is as high as 125 K and the band splitting energy around M is as large as 70 meV. This is consistent with the results of FeSe single crys-

tal, where T_{nem} is ~90 K and no band folding was observed down to 5K [20–27]. One may argue that the FeSe system might have strong spin fluctuation without long-range magnetic order, due to the fine balance of the exchange interaction [39] or spin/charge fluctuations [40]. However, this seems highly unlikely considering the existence of nematicity without long-range magnetic order in the large parameter space of the layer-dependence of the FeSe thin film, where T_{nem} changes from 170 K to 125 K when the thickness of the film increases from 2ML to 35ML [33]. Based on all these facts, the electronic nematicity here is unlikely of spin-nematic origin. This is further supported by the NMR and thermodynamic studies on FeSe single crystal, which also point out the non-magnetic origin of the nematic state [21, 22].

Ruling out the spin-nematicity scenario, let us consider the possibility of orbital ordering. Such a scenario could naturally explain the absence of magnetic ordering in FeSe by assuming a weak coupling between the spin and orbital/lattice. However, the on-site energy difference between the d_{xz} and d_{yz} orbitals would only lead to a band shift that is momentum independent. Therefore, the on-site ferro-orbital ordering alone cannot account for the nontrivial momentum dependence of the band reconstruction observed here.

The non-trivial momentum dependent band reconstruction requires further theoretical understanding. One possible explanation is the orbital-dependent band renormalization. When entering the nematic state, the C4 rotational symmetry breaking does not occur in the orbital occupation. Instead, the anisotropy occurs in the hopping of d_{xz}, d_{xy} and d_{xy} orbitals. The hopping anisotropy between Γ-M_X and Γ-M_Y directions renormalize the bands of d_{yz}, d_{yz} and d_{xy} orbitals differently, resulting in the non-trivial shift of bands at Γ and M. The huge hopping anisotropy cannot originate purely from the lattice distortion, because the change of lattice constant is too small to account for such a large energy scale [5]. The itinerant orbital ordering, the coupling between spin and orbital degree of freedoms, and the role of selenium anion may need to be considered [16, 41].

Finally, the fact that such a huge anisotropy persists down to the lowest measurement temperature raises an important question of how such a nematic order coexists and interacts with superconductivity. Comparing with the FeSe single crystal, the T_{nem} is enhanced to 125 K and no superconductivity has been observed in 35ML FeSe thin film indicating a competition between the nematic order and superconductivity. On the other hand, we note that the observed nematic order is robust in all multilayer FeSe thin films down to 2ML, with T_{nem} as high as 170 K in the 2ML film [33]. In contrast, no signature of nematic order, i.e., the orbital anisotropy, has been detected in the 1ML FeSe that holds the record T_c in all iron-based superconductors [31, 33]. The natural question is how such a strong nematic order in multilayer FeSe is completely suppressed in 1ML FeSe. Is it due to strong coupling between the substrate and FeSe that prevents the 1ML FeSe from going through the nematic/structural transition, or due to the heavy electron doping that suppresses the nematic order and thereby promote the superconductivity? The more important question may be whether there exist strong nematic fluctuations in 1ML FeSe with the complete suppression of nematic order. The answer to this question is intimately related to the pairing mechanism in 1ML FeSe, which is an intensely debated topic in the field. Further investigations are required to elucidate these issues.

CONCLUSION

In conclusion, we report the temperature evolution of electronic band structure in FeSe thin film. The system enters the nematic state at 125 K, while the signature of magnetic order was not observed at the lowest measurement temperature. All the d_{xz}, d_{yz}, d_{xy} orbitals participate in the band reconstruction in nematic state. The energy splitting of the d_{xz}/d_{yz} bands shows non-trivial momentum dependence and the d_{xy} bands split at the M point with a comparable energy scale. Our result exclude the on-site ferro-orbital ordering as the driving force for the nematicity. Instead, anisotropy occurs in the hopping of all d_{xz}, d_{yz}, d_{xy} orbitals. Its origin holds the key in understanding the nematicity and calls for further theoretical and experimental studies.

ACKNOWLEDGMENTS

We thank Fa Wang, Dung-Hai Lee, and Jiangping Hu for valuable discussions. ARPES experiments were performed at the Stanford Synchrotron Radiation Lightsource and the Advanced Light Source, which are both operated by the Office of Basic Energy Sciences, U.S. Department of Energy. The Stanford work is supported by the US DOE, Office of Basic Energy Science, Division of Materials Science and Engineering, under award number DE-AC02-76SF00515.

* Electronic address: zxshen@stanford.edu
† Electronic address: dhlu@slac.stanford.edu

[1] Eduardo Fradkin, Steven A. Kivelson, Michael J. Lawler, James P. Eisenstein, and Andrew P. Mackenzie, Annu. Rev. Cond. Matt. Phys. **1**, 153 (2010).
[2] I. R. Fisher, L. Degiorgi, and Z. X. Shen, Rep. Prog. Phys. **74**, 124506 (2011).
[3] T.-M. Chuang, M. P. Allan, Jinho Lee, Yang Xie, Ni Ni, S. L. Bud′ko, G. S. Boebinger, P. C. Canfield, and J. C. Davis, Science **327**, 181 (2010).
[4] Jiun-Haw Chu, James G. Analytis, Kristiaan De Greve, Peter L. McMahon, Zahirul Islam, Yoshihisa Yamamoto, and Ian R. Fisher, Science **329**, 824 (2010).
[5] Ming Yi, Donghui Lu, Jiun-Haw Chu, James G. Analytis, Adam P. Sorini, Alexander F. Kemper, Brian Moritz, Sung-Kwan Mo, Rob G. Moore, Makoto Hashimoto, Wei-Sheng Lee, Zahid Hussain, Thomas P. Devereaux, Ian R. Fisher, and Zhi-Xun Shen, Proc. Natl. Acad. Sci. **108**, 6878 (2011).

[6] Jiun-Haw Chu, Hsueh-Hui Kuo, James G. Analytis, and Ian R. Fisher, Science **337**, 710 (2012).

[7] R. Daou, J. Chang, David LeBoeuf, Olivier Cyr-Choiniere, Francis Laliberte, Nicolas Doiron-Leyraud, B. J. Ramshaw, Ruixing Liang, D. A. Bonn, W. N. Hardy, and Louis Taillefer, Nature **463**, 519 (2010).

[8] Y. Kohsaka, C. Taylor, K. Fujita, A. Schmidt, C. Lupien, T. Hanaguri, M. Azuma, M. Takano, H. Eisaki, H. Takagi, S. Uchida, and J. C. Davis, Science **315**, 1380 (2007).

[9] M. J. Lawler, K. Fujita, Jhinhwan Lee, A. R. Schmidt, Y. Kohsaka, Chung Koo Kim, H. Eisaki, S. Uchida, J. C. Davis, J. P. Sethna, and Eun-Ah Kim, Nature **466**, 347 (2010).

[10] T. A. Maier and D. J. Scalapino, arXiv: 1405.5238.

[11] S. Lederer, Y. Schattner, E. Berg, and S. A. Kivelson, Phys. Rev. Lett. **114**, 097001 (2015).

[12] Jun Zhao, Q. Huang, Clarina de la Cruz, Shiliang Li, J. W. Lynn, Y. Chen, M. A. Green, G. F. Chen, G. Li, Z. Li, J. L. Luo, N. L. Wang, and Pengcheng Dai, Nat. Mater. **7**, 953 (2008).

[13] Weicheng Lv, Jiansheng Wu, and Philip Phillips, Phys. Rev. B **80**, 224506 (2009).

[14] C. C. Chen, J. Maciejko, A. P. Sorini, B. Moritz, R. R. P. Singh, and T. P. Devereaux, Phys. Rev. B **82**, 100504(R) (2010).

[15] Chi-Cheng Lee, Wei-Guo Yin, and Wei Ku, Phys. Rev. Lett. **103**, 267001 (2009).

[16] Su Yuehua, Liao Haijun, and Li Tao, J. Phys.: Condens. Matter. **27**, 105702 (2015).

[17] M. Daghofer and A. Fischer, Superconductor Science and Technology **25**, 084003 (2012).

[18] Chen Fang, Hong Yao, Wei-Feng Tsai, JiangPing Hu, and Steven A. Kivelson, Phys. Rev. B **77**, 224509 (2008).

[19] R. M. Fernandes, A. V. Chubukov, J. Knolle, I. Eremin, and J. Schmalian, Phys. Rev. B **85**, 024534 (2012).

[20] S. Medvedev, T. M. McQueen, I. A. Troyan, T. Palasyuk, M. I. Eremets, R. J. Cava, S. Naghavi, F. Casper, V. Ksenofontov, G. Wortmann, and C. Felser, Nat. Mater. **8**, 630 (2009).

[21] A. E. Böhmer, T. Arai, F. Hardy, T. Hattori, T. Iye, T. Wolf, H. v. Löhneysen, K. Ishida, and C. Meingast, Phys. Rev. Lett. **114**, 027001 (2015).

[22] S. H. Baek, D. V. Efremov, J. M. Ok, J. S. Kim, Jeroen van den Brink, and B. Büchner, Nat. Mater. **14**, 210 (2015).

[23] P. Zhang, T. Qian, P. Richard, X. P. Wang, H. Miao, B. Q. Lv, B. B. Fu, T. Wolf, C. Meingast, X. X. Wu, Z. Q. Wang, J. P. Hu, and H. Ding, Phys. Rev. B **91**, 214503 (2015).

[24] K. Nakayama, Y. Miyata, G. N. Phan, T. Sato, Y. Tanabe, T. Urata, K. Tanigaki, and T. Takahashi, Phys. Rev. Lett. **113**, 237001 (2014).

[25] T. Shimojima, Y. Suzuki, T. Sonobe, A. Nakamura, M. Sakano, J. Omachi, K. Yoshioka, M. Kuwata-Gonokami, K. Ono, H. Kumigashira, A. E. Bhmer, F. Hardy, T. Wolf, C. Meingast, H. v Lhneysen, H. Ikeda, and K. Ishizaka, Phys. Rev. B **90**, 121111 (2014).

[26] M. D. Watson, T. K. Kim, A. A. Haghighirad, N. R. Davies, A. McCollam, A. Narayanan, S. F. Blake, Y. L. Chen, S. Ghannadzadeh, A. J. Schofield, M. Hoesch, C. Meingast, T. Wolf, and A. I. Coldea, Phys. Rev. B **91**, 155106 (2015).

[27] Y. Suzuki, T. Shimojima, T. Sonobe, A. Nakamura, M. Sakano, H. Tsuji, J. Omachi, K. Yoshioka, M. Kuwata-Gonokami, T. Watashige, R. Kobayashi, S. Kasahara, T. Shibauchi, Y. Matsuda, Y. Yamakawa, H. Kontani, and K. Ishizaka, Phys. Rev. B **92**, 205117 (2015).

[28] Shiliang Li, Clarina de la Cruz, Q. Huang, G. F. Chen, T. L. Xia, J. L. Luo, N. L. Wang, and Pengcheng Dai, Phys. Rev. B **80**, 020504 (2009).

[29] M. Yi, D. H. Lu, R. G. Moore, K. Kihou, C. H. Lee, A. Iyo, H. Eisaki, T. Yoshida, A. Fujimori, and Z. X. Shen, New J. Phys. **14**, 073019 (2012).

[30] Y. Zhang, C. He, Z. R. Ye, J. Jiang, F. Chen, M. Xu, Q. Q. Ge, B. P. Xie, J. Wei, M. Aeschlimann, X. Y. Cui, M. Shi, J. P. Hu, and D. L. Feng, Phys. Rev. B **85**, 085121, (2012).

[31] Xu-Cun Ma, Li-Li Wang, Xi Chen, and Qi-Kun Xue, Chin. Phys. B **22**, 86801 (2013).

[32] W. Li, Y. Zhang, J. J. Lee, H. Ding, M. Yi, Z. Li, P. Deng, K. Chang, S.-K. Mo, M. Hashimoto, D. H. Lu, X. Chen, R. G. Moore, Q.-K. Xue, and Z.-X. Shen, arXiv:1509.01892

[33] Shiyong Tan, Yan Zhang, Miao Xia, Zirong Ye, Fei Chen, Xin Xie, Rui Peng, Difei Xu, Qin Fan, Haichao Xu, Juan Jiang, Tong Zhang, Xinchun Lai, Tao Xiang, Jiangping Hu, Binping Xie, and Donglai Feng, Nat. Mater. **12**, 634, (2013).

[34] V. Brouet, M. F. Jensen, P.-H. Lin, A. Taleb-Ibrahimi, P. Le Fèvre, F. Bertran, C. H. Lin, W. Ku, A. Forget, and D. Colson, Phys. Rev. B **86**, 075123 (2012).

[35] M. Yi, Z. K. Liu, Y. Zhang, R. Yu, J. X. Zhu, J. J. Lee, R. G. Moore, F. T. Schmitt, W. Li, S. C. Riggs, J. H. Chu, B. Lv, J. Hu, M. Hashimoto, S. K. Mo, Z. Hussain, Z. Q. Mao, C. W. Chu, I. R. Fisher, Q. Si, Z. X. Shen, and D. H. Lu, Nat. Comm. **6**, 7777 (2015).

[36] Ningning Hao and Jiangping Hu, Topological Phases in the Single-Layer FeSe. Phys. Rev. X **4**, 031053 (2014).

[37] Z. R. Ye, C. F. Zhang, H. L. Ning, W. Li, L. Chen, T. Jia, M. Hashimoto, D. H. Lu, Z.-X. Shen, and Y. Zhang, arXiv: 1512.02526.

[38] S. Graser, T. A. Maier, P. J. Hirschfeld, and D. J. Scalapino, New J. Phys. **11**, 025016 (2009).

[39] Fa Wang, Steven A. Kivelson, and Dung-Hai Lee, Nat. Phys. **11**, 959 (2015).

[40] Andrey V. Chubukov, Rafael M. Fernandes, and Joerg Schmalian, Phys. Rev. B **91**, 201105 (2015).

[41] Seiichiro Onari, Youichi Yamakawa, and Hiroshi Kontani, Phys. Rev. Lett. **116**, 227001 (2016).